DOI: 10.1478/AAPP.97S2A4

AAPP | Atti della Accademia Peloritana dei Pericolanti
Classe di Scienze Fisiche, Matematiche e Naturali
ISSN 1825-1242

Vol. 97, No. S2, A4 (2019)

THE TWO-FLUID EXTENDED MODEL OF SUPERFLUID HELIUM

LUCA GALANTUCCI [a], MICHELE SCIACCA [b c *] AND DAVID JOU [d e]

ABSTRACT. In this paper we perform the first numerical comparison between the two main existing models of superfluid helium: the two-fluid model proposed by Landau and the one-fluid extended model proposed from the extended thermodynamics. The numerical experiments in this paper regard the profiles of the so-called normal and superfluid components in 2D counterflow turbulence.

1. Introduction

Superfluid helium exhibits some peculiarities, which make it different from classical fluids. One of most interesting behaviour of superfluid helium is heat transfer in counterflow experiments, characterized by no net matter flow but only heat transport. There, a low heat flux inside the channel, less than a critical value ($q < q_c$), makes the temperature gradient so small that it cannot be measured, so indicating that the superfluid helium has an extremely high thermal conductivity (Tisza 1938; Landau 1941; London 1954; Khalatnikov 2018).

In the middle of the previous century, Landau and Tisza proposed the two-fluid model, which sees superfluid helium made by two components, the normal component (a classical viscous fluid leading the whole entropy of superfluid helium) and the superfluid component (a viscousless fluid) (Tisza 1938; Landau 1941). The two-fluid model is the most famous and most used model nowadays even though Landau himself observed that the two-fluid model is not completely satisfactory from a theoretical point of view because the two components cannot exist separately. For this reason some authors (Putterman 1974; Lebon and Jou 1979; Atkin and Fox 1984) showed that the results of the theory can be established also through the use of the conventional variables of a single fluid, but assuming the existence of a further vector field which can be related to the velocity of the superfluid component v_i^s in the two-fluid model.

Recently, the one-fluid extended model of superfluid helium has been proposed (Mongiovì 1991, 1992, 1993a,c, 2000; Mongiovì *et al.* 2018), which is based on the framework of Extended Thermodynamics (E.T.) (Mueller and Ruggeri 1998; Lebon *et al.* 2008; Jou *et al.* 2010, 2011). This model describes the anomalous behaviour of liquid helium II as well, and the relative motion between normal and superfluid components is described by an internal variable, that macroscopically can be put in relation with the heat flux.

As a first comparison between these two models, the one-fluid extended model sees only a single fluid, rather than two physically different fluids, with the dynamics of the heat flux (whose relaxation time is very long) as a further internal degree of freedom arising from the relative motion of the two fluids. The two fields $\mathbf{v}$ and $\mathbf{q}$ (the barycentric velocity and the heat flux) used in the one-fluid extended model are directly measurable, whereas the two fields $\mathbf{v}_n$ and $\mathbf{v}_s$ (the velocities of the normal component and of the superfluid component, respectively) in the two-fluid model are only indirectly measured, usually from the measurements of $\mathbf{q}$ and $\mathbf{v}$. In contrast, the two-fluid model has a more explicit microscopic view of what is going on in the physical process. For the sake of completeness, a brief microscopical interpretation of the one-fluid model has been carried out in the recent review paper (Mongiovì *et al.* 2018).

In the framework of the one-fluid extended model the two fundamental variables are the velocity $\mathbf{v}$ and the heat flux $\mathbf{q}$, apart from the density ρ and the temperature T related to the internal energy of the fluid. In this model two fields, with the dimensions of velocity naturally arise, which we set $\mathbf{u}^{(n)}$ and $\mathbf{u}^{(s)}$: the first can be interpreted as the normal component speed and the second as the superfluid component speed (Mongiovì *et al.* 2018), which we can still call two-fluid extended model. The two-fluid version of the one-fluid extended model allows a better comparison between the two existing models and the experiments. For instance, the two-fluid extended model allows that an amount of entropy can be carried by the superfluid component, as stated by Putterman (1974).

According to the two-fluid model, counterflow experiments are characterized by a flow of the normal component, carrying the entropy and temperature out from the heater, and by a flow of the superfluid components counterflowing in the opposite direction and towards the heater, in such a way that the average mass flow accross any transversal section of the channel is zero. In terms of the one-fluid extended model, instead, the counterflow experiments are characterized by the motion of the heat flow with a null average barycentric velocity across any transversal section of the channel.

In these experiments, when the heat flux exceeds a critical value q_c, vortex filaments appear with a quantized circulation $\kappa = h/m_4$ (with h the Planck constant and m_4 the mass of ^{4}He atom, with $\kappa \simeq 9.97\ 10^{-4}\text{cm}^2/\text{s}$) (Vinen 1957a,b,c, 1958).

In (Jou and Sciacca 2013) the critical value q_c for the appearance of quantum turbulence (tangle of quantized vortices) is related to a critical value of a quantum Reynolds number Rey_q defined as $Rey_q = \frac{q}{\rho s T}\frac{d}{\kappa}$, with d the diameter of the tube and ρs the entropy density per unit volume. The critical value of Rey_q depends on temperature and it is of the order of 10^2.

The presence of quantized vortices produces a damping force: the mutual friction force. It is microscopically seen to be the result from the collision of the quasiparticles (phonons and rotons) with the array of vortex lines (Donnelly 1991; Barenghi *et al.* 2001; Nemirovskii 2013). Thus, it is a function of the direction of the quasiparticles drift velocity with respect to the vortex line: maximum when the direction is perpendicular to the vortex line and minimum when it is parallel to the line.

The paper is organized as follows: Section **2** deals with the mathematical model used in the paper, in particular in subsection **2.1** we recall some details which lead the one-fluid extended model to the usual two-fluid model, and in subsection **2.2** we consider the 2D

model applied to a counterflow channel; Section **3** is devoted to the numerical results and Section **4** to the Conclusions.

2. The mathematical model

In this section we briefly recall the main fields of the two models, the one-fluid extended model proposed by using Extended Thermodynamics and the two-fluid model proposed by Tisza and Landau.

2.1. From the one-fluid extended model to a two-fluid model. In terms of the Extended Thermodynamics, the fundamental fields needed to describe the dynamical behavior of helium II are the two scalar fields ρ and T and the two vector fields $\mathbf{v}$ and $\mathbf{q}$.

The field equations of helium II, in the presence of dissipation and in the absence of the fluxes of higher order, are (Mongiovì 1993b; Mongiovì *et al.* 2018)

$$\begin{cases} \dot{\rho} + \rho \nabla \cdot \mathbf{v} = 0 \\ \rho \dot{\mathbf{v}} + \nabla p - \nabla \cdot \mathbf{P_v} = 0 \\ \rho \dot{\varepsilon} + \nabla \cdot \mathbf{q} + p \nabla \cdot \mathbf{v} - \mathbf{P_v} : \nabla \mathbf{v} = 0 \\ \dot{\mathbf{q}} + \zeta \nabla T + \zeta \nabla \cdot \mathbf{P_q} = \sigma^{\mathbf{q}} \end{cases} \tag{1}$$

where p is the pressure, ε is the energy density, $\zeta = \lambda_1/\tau_1$ with λ_1 thermal conductivity and τ the relaxation time, that characterizes the second-sound velocity V_2, given by $V_2^2 = \frac{\zeta}{\rho c_V}$ and $\mathbf{P_v}$ and $\mathbf{P_q}$ given by:

$$\mathbf{P_v} = \lambda_0 \left[\nabla \cdot \mathbf{v} - \beta' T \nabla \cdot \mathbf{q}\right] \mathbf{U} + 2\eta \left[\langle \nabla \mathbf{v} \rangle - \beta T \langle \nabla \mathbf{q} \rangle\right], \tag{2}$$

$$\mathbf{P_q} = \lambda_0 \beta' T^2 \left[\nabla \cdot \mathbf{v} - \beta' T \nabla \cdot \mathbf{q}\right] \mathbf{U} + 2\eta \beta T^2 \left[\langle \nabla \mathbf{v} \rangle - \beta T \langle \nabla \mathbf{q} \rangle\right]. \tag{3}$$

where coefficients β and β' are negative and take into account of the dissipation of thermal origin and $\langle \ldots \rangle$ stands for the deviatoric part of the tensors.

The production term σ^q in the turbulent regime is

$$\sigma^q = -\frac{1}{\tau_1}\mathbf{q} - KL\mathbf{q} \tag{4}$$

where $K = \frac{1}{3}\kappa B_{HV}$, B_{HV} being the dimensionless Hall-Vinen friction coefficient (Vinen 1957b), and L is the vortex line length per unit volume.

From the one-fluid extended model, an extended two-fluid model naturally arises. Indeed, consider the propagation of harmonic plane waves of the fields $\mathscr{U} = (p, T, v_i, q_i)$ having the form:

$$\mathscr{U} = \mathscr{U}_0 + \tilde{\mathscr{U}} e^{i(Kn_j x_j - \omega t)} \tag{5}$$

where $\mathscr{U}_0 = (p_0, T_0, 0, 0)$, $\tilde{\mathscr{U}} = (\tilde{p}, \tilde{T}, \tilde{v}_i, \tilde{q}_i)$, ω the angular frequency, and $K = k_r + ik_s$ is the complex wave number. The oversigned-tilde quantities denote small amplitudes whose products can be neglected. Inserting (5) in the linearized field equations (1), we can

investigate on the propagation of the longitudinal and transversal modes (Mongiovì 1993b). In particular, the analysis of the transversal mode leads in a direct way to a two-fluid model.

In the first transversal mode, the vector field:

$$\mathbf{u}^{(n)} = \mathbf{v} - \beta T \mathbf{q} \tag{6}$$

is almost zero, whence in the second transversal mode the vector

$$\mathbf{u}^{(s)} = \mathbf{v} + \frac{\beta T}{P-1}\mathbf{q} \tag{7}$$

(with $P = 1 + \rho\beta^2 T^3 \zeta$) is almost zero. Thus, the first transverse mode corresponds to a very slow relaxation involving only $\mathbf{u}^{(s)}$, the second mode corresponds to perturbations of $\mathbf{u}^{(n)}$ which are attenuated within a small number of wavelenghts.

From (6) and (7) we find

$$\mathbf{v} = \frac{P-1}{P}\mathbf{u}^{(s)} + \frac{1}{P}\mathbf{u}^{(n)}, \qquad \mathbf{q} = \frac{1}{\beta T}\frac{P-1}{P}[\mathbf{u}^{(s)} - \mathbf{u}^{(n)}]. \tag{8}$$

The first relation (8) suggests the introduction of two scalar fields, $\rho^{(s)}$ and $\rho^{(n)}$, associated with $\mathbf{u}^{(s)}$ and $\mathbf{u}^{(n)}$, which can be interpreted as the "densities" of the superfluid and normal components in helium II. Specifically, they are given as

$$\frac{\rho^{(s)}}{\rho} = \frac{P-1}{P}, \qquad \frac{\rho^{(n)}}{\rho} = \frac{1}{P}. \tag{9}$$

Examining the "convective" terms of the entropy flux $\mathbf{J}^S$; from equation of entropy flux it follows that

$$s^{(s)} = s + \frac{1}{\rho\beta T^2} = s\frac{\rho^{(s)}}{\rho}\left(1 - \frac{\beta^*}{\beta}\right), \qquad s^{(n)} = s - \frac{\rho^{(s)}}{\rho^{(n)}\rho\beta T^2}, \tag{10}$$

can be interpreted as the entropy of the superfluid and of the normal component, respectively (Mongiovì *et al.* 2018).

The small entropy $s^{(s)}$ carried by superfluid component influences many dynamical and thermodynamical properties of liquid helium II, as for instance speeds and attenuations of the first and second sounds. From (9) and (10), taking in mind $\beta^* := -(\rho s T^2)^{-1}$ one deduces

$$\frac{s_s}{s} = 1 - \frac{\beta^*}{\beta} \tag{11}$$

which implies that the superfluid entropy influences only quantities depending explicitly on parameter β.

Using relation (11) one obtains:

$$\mathbf{u}^{(n)} = \mathbf{v} + \frac{1}{\rho(s-s_s)T}\mathbf{q}, \qquad \mathbf{u}^{(s)} = \mathbf{v} - \frac{s-s_s}{\zeta}\mathbf{q}. \tag{12}$$

Note that if $s^{(s)} = 0$, namely, β takes the particular value $\beta^* := -(\rho s T^2)^{-1}$ then the entropy flux will depend only on the $\mathbf{u}^{(n)}$ and the fields $\mathbf{u}^{(n)}$ and $\mathbf{u}^{(s)}$ coincide with $\mathbf{v}_n$ and $\mathbf{v}_s$:

$$\mathbf{u}^{(n)} = \mathbf{v} + \frac{1}{\rho T s}\mathbf{q} = \mathbf{v}_n, \qquad \mathbf{u}^{(s)} = \mathbf{v} - \frac{s}{\zeta}\mathbf{q} = \mathbf{v}_s \tag{13}$$

and if we put

$$\zeta = \rho \frac{\rho_s}{\rho_n} T s^2 \tag{14}$$

the linearized equations of the one-fluid model, in the absence of dissipative phenomena, are identical with those of the original Landau two-fluid model (Mongiovì 1991).

Note that from the above expressions, the superfluid entropy modifies the speeds of normal and superfluid components, and in particular one concludes that:

$$\mathbf{u}^{(n)} = \mathbf{v}_n + \frac{1}{\rho s T}\left(\frac{1}{1-\frac{s_s}{s}} - 1\right)\mathbf{q}, \qquad \mathbf{u}^{(s)} = \mathbf{v}_s + \frac{s_s}{\zeta}\mathbf{q}. \tag{15}$$

Note that the presence of small amount of entropy associated to the superfluid component modifies the velocities $\mathbf{u}^{(n)}$ and $\mathbf{u}^{(s)}$ in such a way they assume values higher than the corresponding ones in the usual two-fluid model.

In counterflow experiments, the further condition $\overline{\mathbf{v}} = 0$ (where $\overline{\mathbf{v}}$ is the averaged value of the velocity field $\mathbf{v}$ accross the channel) implies that expressions (12) become $\overline{\mathbf{q}} = \rho(s - s_s) T \overline{\mathbf{u}}^{(n)}$ and $\frac{s_s}{\zeta}\overline{\mathbf{q}} = -\frac{s_s}{s-s_s}\overline{\mathbf{u}}^{(s)}$, and hence that

$$\overline{\mathbf{u}}^{(s)} = \left(1 - \frac{s_s}{s}\right)\overline{\mathbf{v}}_s \qquad \text{and} \qquad \overline{\mathbf{u}}^{(n)} = \frac{s}{s-s_s}\overline{\mathbf{v}}_n \tag{16}$$

If $s_s = 0.02s$ (Putterman 1974) then $\overline{\mathbf{u}}^{(s)} = 0.98\overline{\mathbf{v}}_s$ and $\overline{\mathbf{u}}^{(n)} = 1.02\overline{\mathbf{v}}_n$.

As shown in Mongiovì (2001), neither the velocity nor the attenuation of first sound depend perceptibly on s_s. In contrast, the presence of entropy associated with superfluid component seems to influence second sound velocity and attenuation. In fact, one can write:

$$V_2^2 = \frac{\rho^{(s)}}{\rho^{(n)}}\frac{T}{c_V}(s - s_s)^2. \tag{17}$$

Note that equation (17) allows us to determine the small entropy s_s associated to superfluid component, only if the quantity $\rho^{(s)}/\rho^{(n)}$ can be calculated independently.

Relations (8) can be written (Mongiovì 2001; Mongiovì *et al.* 2018)

$$\mathbf{v} = \frac{\rho^{(n)}}{\rho}\mathbf{u}^{(n)} + \frac{\rho^{(s)}}{\rho}\mathbf{u}^{(s)}, \tag{18}$$

$$\mathbf{q} = \rho^{(s)} T (s - s_s)(\mathbf{u}^{(n)} - \mathbf{u}^{(s)}). \tag{19}$$

with $\frac{\rho^{(n)}}{\rho} = \frac{\zeta}{\zeta + \rho T (s-s_s)^2}$ and $\frac{\rho^{(s)}}{\rho} = \frac{\rho T (s-s_s)^2}{\zeta + \rho T (s-s_s)^2}$, which also show the role of s_s. The presence of the superfluid entropy modifies the ratios $\frac{\rho^{(n)}}{\rho}$ and $\frac{\rho^{(s)}}{\rho}$ in such a way that $\rho^{(n)} \geq \rho_n$ and $\rho^{(s)} \leq \rho_s$, because $\frac{\rho}{\rho^{(n)}} = 1 + \frac{\rho T s^2}{\zeta}\left(1 - \frac{s_s}{s}\right)^2 \leq 1 + \frac{\rho T s^2}{\zeta} = \frac{\rho}{\rho_n}$ and hence

$\rho^{(n)} \geq \rho_n$. The second conclusion follows from the relations $\rho^{(n)} + \rho^{(s)} = \rho = \rho_n + \rho_s$. Moreover, if $s_s = 0.02s$ then $\frac{\rho}{\rho^{(n)}} = 1 + \left(\frac{\rho}{\rho_n} - 1\right)\left(1 - \frac{s_s}{s}\right)^2 = 1 + 0.96\left(\frac{\rho}{\rho_n} - 1\right)$ and $\frac{\rho}{\rho^{(s)}} = 1 + \left(\frac{\rho}{\rho_s} - 1\right)\frac{1}{\left(1-\frac{s_s}{s}\right)^2} = 1 + 1.04\left(\frac{\rho}{\rho_s} - 1\right)$.

In terms of $s - s^{(s)}$ and assuming $\beta = \beta'$, the two latter equations in system (1) become:

$$\frac{\partial}{\partial t}\mathbf{u}^{(n)} + (\mathbf{v}\cdot\nabla)\mathbf{u}^{(n)} = -\frac{1}{\rho}\nabla p - \frac{\rho^{(s)}}{\rho^{(n)}}(s - s^{(s)})\nabla T + \frac{\lambda_0}{\rho^{(n)}}\nabla(\nabla\cdot\mathbf{u}^{(n)}) + \\ + \frac{\eta}{\rho^{(n)}}\nabla^2\mathbf{u}^{(n)} + \frac{1}{\tau_1}\frac{\rho^{(s)}}{\rho}(\mathbf{u}^{(s)} - \mathbf{u}^{(n)}), \tag{20}$$

$$\frac{\partial}{\partial t}\mathbf{u}^{(s)} + (\mathbf{v}\cdot\nabla)\mathbf{u}^{(s)} = -\frac{1}{\rho}\nabla p + (s - s^{(s)})\nabla T - \frac{1}{\tau_1}\frac{\rho^{(n)}}{\rho}(\mathbf{u}^{(s)} - \mathbf{u}^{(n)}), \tag{21}$$

where we have considered the relation (14) with $(s - s^{(s)})$ instead of s.

Neglecting terms proportional to $1/\tau_1$ (because τ_1 is very high in superfluid helium) in the equations (20) and (21) we have

$$\frac{\partial\mathbf{u}^{(n)}}{\partial t} + (\mathbf{v}\cdot\nabla)\mathbf{u}^{(n)} = -\frac{1}{\rho}\nabla p - \frac{\rho^{(s)}}{\rho^{(n)}}(s - s^{(s)})\nabla T + \frac{\lambda_0}{\rho^{(n)}}\nabla(\nabla\cdot\mathbf{u}^{(n)}) + \frac{\eta}{\rho^{(n)}}\nabla^2\mathbf{u}^{(n)}, \tag{22}$$

$$\frac{\partial\mathbf{u}^{(s)}}{\partial t} + (\mathbf{v}\cdot\nabla)\mathbf{u}^{(s)} = -\frac{1}{\rho}\nabla p + (s - s^{(s)})\nabla T, \tag{23}$$

Instead, in the usual Landau-Tisza two-fluid model we have

$$\frac{\partial}{\partial t}\mathbf{v}_n + (\mathbf{v}_n\cdot\nabla)\mathbf{v}_n = -\frac{1}{\rho}\nabla p - \frac{\rho_s}{\rho_n}s\nabla T + \frac{\lambda_0}{\rho_n}\nabla(\nabla\cdot\mathbf{v}_n) + \frac{\eta}{\rho_n}\nabla^2\mathbf{v}_n, \tag{24}$$

$$\frac{\partial}{\partial t}\mathbf{v}_s + (\mathbf{v}_s\cdot\nabla)\mathbf{v}_s = -\frac{1}{\rho}\nabla p + s\nabla T, \tag{25}$$

which differ from equations (22) and (23) for the entropy of the superfluid component $s^{(s)}$ and for the velocity $\mathbf{v}$, instead of $\mathbf{v}_n$ and $\mathbf{v}_s$, in the convective term. Note that expressions (22) and (23) are found after neglecting nonlinear terms of higher order, which may not be negligible in general, and which make the two-fluid extended model more exhaustive than the usual two-fluid model.

A further difference between the hydrodynamical model, the two-fluid model, and the thermodynamical one, the one-fluid extended model, occurs at very low temperature (less than 1 K), when the density of the quasiparticles (rotons and photons) inside superlfuid helium is practically null. This means that the dynamics of these quasiparticles at very low temperature becomes ballistic and the two-fluid model cannot be used more for superfluid helium. The one-fluid extended model is instead valid in the ballistic regime, and hence at very low temperature (Sciacca *et al.* 2014).

2.2. The 2D model. In this subsection we follow the general lines of the paper (Galantucci *et al.* 2015), which considers an infinitely long two–dimensional channel of width D, with x and y the directions along and across the channel, respectively ($-D/2 \leq y \leq D/2$ and periodic boundary conditions imposed at $x = 0$ and $x = L_x$). More details about the numerical code can be found in (Galantucci *et al.* 2011; Galantucci *et al.* 2015). Our numerical experiments will be applied to a counterflow channel (heat flow without mass flow) in terms of the two-fluid extended model (22) and (23) obtained from the one-fluid extended model.

The calculation will mainly regard the dynamics of the vortex points over the channel (which correspond ideally to the dynamics of the vortex lines in three-dimensions) and the dynamical equation for the normal component. The velocity field of the superfluid component will be instead obtained by means of the superfluid field generated by all vortex points and the counterflow condition $\rho^{(n)}\overline{\mathbf{u}}^{(n)} + \rho^{(s)}\overline{\mathbf{u}}^{(s)} = 0$, where $\overline{\cdots}$ indicates channel-averaged quantities.

More in details, the dynamics of the normal component is given by equations $\nabla \cdot \mathbf{u}^{(n)} = 0$ and

$$\frac{\partial \mathbf{u}^{(n)}}{\partial t} + (\mathbf{v}\cdot\nabla)\mathbf{u}^{(n)} = -\frac{1}{\rho}\nabla p - \frac{\rho^{(s)}}{\rho^{(n)}}(s - s^{(s)})\nabla T + \frac{\eta}{\rho^{(n)}}\nabla^2\mathbf{u}^{(n)} + \frac{1}{\rho^{(n)}}\mathbf{F}_{ns}, \tag{26}$$

where the mutual friction term $\mathbf{F}_{ns}$ has been considered because of the interaction between the normal component and the quantized vortices (Vinen 1957b).

Quantum vortex lines in a two-dimensional channel are described by N vortex–points of circulation κ (half of them have positive circulation and half have negative circulation) and position $\mathbf{r}_j(t) = (x_j(t), y_j(t))$, where $j = 1, \ldots N$.

They move according to the following equation proposed by Schwarz (1988)

$$\begin{aligned} \frac{d\mathbf{r}_j}{dt} &= \mathbf{u}_0^{(s)}(\mathbf{r}_j,t) + \mathbf{u}_i^{(s)}(\mathbf{r}_j,t) \\ &+ \alpha\,\mathbf{s}'_j \times \left(\mathbf{u}^{(n)}(\mathbf{r}_j,t) - \mathbf{u}_0^{(s)}(\mathbf{r}_j,t) - \mathbf{u}_i^{(s)}(\mathbf{r}_j,t)\right) \\ &+ \alpha' \left(\mathbf{u}^{(n)}(\mathbf{r}_j,t) - \mathbf{u}_0^{(s)}(\mathbf{r}_j,t) - \mathbf{u}_i^{(s)}(\mathbf{r}_j,t)\right) \end{aligned} \tag{27}$$

where $\mathbf{s}'_j$ is the unit vector along vortex j (in the positive z direction if the quantum of circulation is $\Gamma_j = \kappa$ and in the negative z direction if instead $\Gamma_j = -\kappa$), α and α' are mutual friction coefficients, depending on the temperature, (Barenghi *et al.* 1983), the field $\mathbf{u}^{(n)}(\mathbf{r}_j,t)$ is the normal fluid velocity at position $\mathbf{r}_j$, $\mathbf{u}_i^{(s)}(\mathbf{r}_j,t) = \sum_{k=1\ldots N}\mathbf{u}_{i,k}^{(s)}(\mathbf{r}_j,t)$ is the superfluid velocity field induced by all N vortex–points at $\mathbf{r}_j$ and $\mathbf{u}_0^{(s)} = (u_{0x}^{(s)}, 0)$ is the superfluid flow which enforces the counterflow condition $\rho^{(n)}\overline{\mathbf{u}}^{(n)} + \rho^{(s)}(\overline{\mathbf{u}}_0^{(s)} + \overline{\mathbf{v}_{si}}) = 0$ at each channel cross-section (for futher details see Galantucci *et al.* (2015)). This means that we do not need to solve equation (25) to find the superfluid velocity $\mathbf{u}^{(s)}$ in a point $\mathbf{r}$, but it is given by the sum of the contribution of each vortex point $\mathbf{u}_i^{(s)}(\mathbf{r})$ and a constant contribution $\mathbf{u}_0^{(s)}$, satisfying the counterflow condition $\rho^{(n)}\overline{\mathbf{u}}^{(n)} + \rho^{(s)}(\overline{\mathbf{u}}_0^{(s)} + \overline{\mathbf{v}_{si}}) = 0$.

The creation and the destruction of vortices in our two–dimensional model is achieved by a "numerical vortex reconnection" procedure described, tested and employed in our previous papers (Galantucci *et al.* 2011; Galantucci and Sciacca 2012, 2014; Galantucci *et al.* 2015; Galantucci *et al.* 2017): a couple of vortex points is removed and then randomly re-inserted in the channel when the distance between the two vortex points of opposite circulation becomes smaller than a critical value ε_1 or when when the distance between a vortex point and a channel wall is less than $\varepsilon_2 = 0.5\varepsilon_1$ (refer to Galantucci *et al.* (2015) and Supplementary Material in Galantucci *et al.* (2017) for further insight on this numerical reconnection model).

The dynamical state of the normal fluid is investigated by applying the vorticity-stream function formulation to (26) equations, obtaining the following set of equations

$$\nabla^2 \Psi = -\omega_n \,, \tag{28}$$

$$\begin{aligned} \frac{\partial \omega_n}{\partial t} + \left(\frac{\rho^{(n)}}{\rho} \frac{\partial \Psi}{\partial y} + \frac{\rho^{(s)}}{\rho} (u_{0x}^{(} s) + u_{0x}^{(s)} \right) + \left(-\frac{\rho^n}{\rho} \frac{\partial \Psi}{\partial x} + u_{iy}^{(s)} \right) \frac{\partial \omega_n}{\partial y} = \\ \nu_n \nabla^2 \omega_n + \frac{1}{\rho_n} \left(\frac{\partial \widetilde{F}^y}{\partial x} - \frac{\partial \widetilde{F}^x}{\partial y} \right) \end{aligned} \tag{29}$$

where $\widetilde{\mathbf{F}}_{ns} = (\widetilde{F}^x, \widetilde{F}^y)$ is the mutual friction force and the stream function Ψ and the normal vorticity ω_n are defined as follows: $\mathbf{u}^{(n)} = (\partial \Psi y, -\partial \Psi x)$, $\omega_n = \nabla \times \mathbf{u}^{(n)}$.

The Cauchy-Dirichlet problem associated to (28) and (29) is:

$$\mathbf{u}^{(n)}(x, \pm D/2) = \mathbf{0} \qquad \forall t;\ \mathbf{u}^{(n)}(x,y)_{|t=0} = \left(-V_{n0} \left[1 - (2y/D)^2 \right], 0 \right)$$

together with the counterflow condition

$$\rho^{(n)} \langle \mathbf{u}^{(n)} \rangle + \rho^{(s)} \langle \mathbf{u}_0^{(s)} + \mathbf{u}_i^{(s)} \rangle = 0. \tag{30}$$

For the mutual friction force $\mathbf{F}_{ns}$ we use the coarse–grained theoretical framework proposed by Hall and Vinen (Hall and Vinen 1956), at lengthscales larger than the average inter-vortex spacing ℓ. For this reason, we distinguish between the fine $(\Delta x, \Delta y)$ grid where $\mathbf{u}^{(n)}$ is numerically determined, and the coarser $(\Delta X, \Delta Y)$ grid on which we define the mutual friction $\widetilde{\mathbf{F}}_{ns}$ given by Hall and Vinen's proposal

$$\widetilde{\mathbf{F}}_{ns} = \alpha \rho_s \widetilde{\widetilde{\omega}}_s \times \left[\widetilde{\omega}_s \times \left(\widetilde{\mathbf{u}}^{(n)} - \widetilde{\mathbf{u}}^{(n)} \right) \right] + \alpha' \rho_s \widetilde{\omega}_s \times \left(\widetilde{\mathbf{u}}^{(n)} - \widetilde{\mathbf{u}}^{(n)} \right), \tag{31}$$

where $\widetilde{\cdot}$ symbols indicate coarse–grained averaged quantities, *i.e.* quantities averaged over coarse grid-cells. After the mutual friction force $\widetilde{\mathbf{F}}_{ns}$ is computed on the coarse grid we interpolate it on the finer grid via a two–dimensional bi–cubic convolution kernel (Keys 1981).

The complete list of parameters employed in our simulation and the physical relevant quantities are reported in Tables 1 and 2, expressed in terms of the following units of length, velocity and time, respectively: $\delta_c = D/2 = 1.0 \times 10^{-1}\,\mathrm{cm}$, $u_c = \kappa/(2\pi\delta_c) = 1.59 \times 10^{-3}\,\mathrm{cm/s}$, $t_c = \delta_c/u_c = 62.79\,\mathrm{s}$. Hereafter all the quantities which we mention are

D	2	T	$1.7K$
L_x	6	ρ_s/ρ_n	3.373
N	3072	ℓ	6.25×10^{-2}

TABLE 1. Physical and numerical parameters employed in the simulations in dimensionless units

Fine grid		Coarse grid	
n_x	192	N_x	48
n_y	64	N_y	16
Δx	3.125×10^{-2}	ΔX	0.125
Δy	3.125×10^{-2}	ΔY	0.125

TABLE 2. Number of grid–points and spacings in dimensionless units of the grids employed in the simulations

dimensionless, unless otherwise stated. The parameters employed in the present simulations, in particular the channel width D, the average inter-vortex spacing ℓ (determined by the number of vortex points N) and the normal fluid volume flow-rate (imposed by the parameter V_{n0}), have been chosen in order to make at least qualitative comparisons with the recent experimental superflow studies performed in Prague (Babuin *et al.* 2012; Babuin *et al.* 2015; Varga *et al.* 2015).

For further numerical details concerning the numerical model employed in order to perform the simulations (integration methods, timesteps, grids characteristics) please refer to (Galantucci *et al.* 2011; Galantucci and Sciacca 2012, 2014; Galantucci *et al.* 2015; Galantucci *et al.* 2017).

3. Results

In this section we present the numerical results obtained by means of the two models, the usual (Landau) and the extended two-fluid models, using the vortex-line density investigated in Galantucci *et al.* (2017). The aim of our numerical simulation is first, in Subsection **3.1**, to compare the results of the two models and second, in Subsection **3.2**, to investigate low viscosity effects by means of the two-fluid extended model.

3.1. Comparison with the usual two-fluid model. In this subsection we consider Helium II counterflows studied by means of the two-fluid models with the parameters reported in Table 1 and 2. The choice of these parameters aims to support our previous results (Galantucci *et al.* 2015), which have been performed with different parameters, and to make our numerical simulations more consistent with the recent experiments (Babuin *et al.* 2012).

In Fig. 1 and 2 the numerical results with the usual and the extended two fluid model are reported, respectively. The figure on the left shows the profile of the velocity of the superfluid (red line) and normal fluid (blue line) components. The latter is compared with the parabolic profile of the Poiseuille flow (blue dotted line). Even though our simulations are bidimensional, both the models mimic succesfully the experiments (Marakov *et al.*

2015). In our simulations, we have not taken into account of the superfluid entropy, which, according to Putterman (Putterman 1974), is extimated of about $s_s = 0.02s$. Taking into account this value of s_s we find that the value of the two velocity have to be modified of the order of $\overline{\mathbf{u}}^{(s)}_{s_s\neq 0} = 0.98\overline{\mathbf{u}}^{(s)}$ and $\overline{\mathbf{u}}^{(n)}_{s_s\neq 0} = 0.98\overline{\mathbf{u}}^{(n)}$, as reported below equation (16). The presence of the superfluid entropy changes the profile of the two components making the normal component a little bit closer to the results of the experiments.

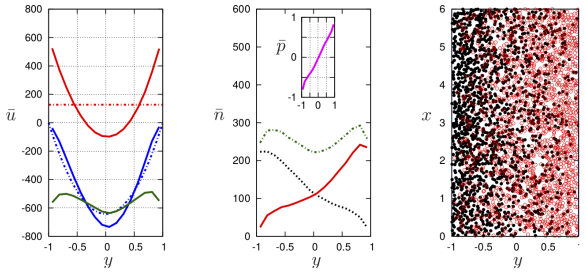

FIGURE 1. Numerical results for the usual (Landau) two fluid model: (left) the profile of superfluid component $\mathbf{v}_s$ (red line), the normal component $\mathbf{v}_n$ (blue line) compared with the Poiseuille profile (blue dotted line), the flat superfluid component $\mathbf{v}_s$ in the absence of vortices (red dotted line) and the counterflow velocity $\mathbf{v}_{ns} = \mathbf{v}_n - \mathbf{v}_s$ (green line); (middle) the number of vortex points per unit area in the channel (green dotted line), the number of positive vortex points per unti area (red line), the number of negative vortex points per unit area (black dotted line) and the polarization $\mathbf{p}$ (purple line); (right) the distribution of the positive (red) and negative (black) vortex points inside the channel when a statistically steady state has been achieved.

From a rough comparison between the results shown in Fig. 1 and 2, we do not notice a strong difference between the results of the two models, apart from that reported above. The explanation is found in the strength of the terms of the equations (22) and (24), in particular in the strength of the term $\left(\frac{\rho^{(s)}}{\rho^{(n)}}\mathbf{u}^{(s)}\cdot\nabla\right)\mathbf{u}^{(n)}$, which is absent in equation (24). For this reason in the next subsection we consider a numerical experiment with lower normal viscosity, which makes this term more relevant.

3.2. Numerical results with low viscosity. In this subsection, we perform a numerical experiment employing the two-fluid extended model with the same parameters as in the previous paragraph, apart from the viscosity which is set equal to $1/5$ of its real value (used in the previous simulations).

The numerical results are shown in Fig. 3. The smaller amount of the viscosity makes the other terms of the equation (22) consequently stronger. Note the net separation of the vortex points in the Fig. 3 (right), caused by the mutual friction force.

4. Conclusions

In this paper we have performed the first numerical comparison between the two existing models of superfluid helium: the usual two-fluid Landau model and the extended two-fluid

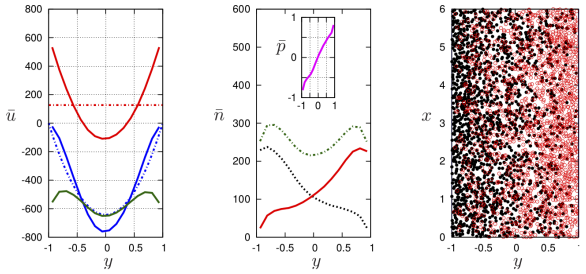

FIGURE 2. Numerical results for the extended two fluid model: (left) the profile of superfluid component $\mathbf{u}^{(s)}$ (red line), the normal component $\mathbf{u}^{(n)}$ (blue line) compared with the Poiseuille profile (blue dotted line), the flat superfluid component $\mathbf{u}^{(s)}$ in the absence of vortices (red dotted line) and the counterflow velocity $\mathbf{u}^{(ns)} = \mathbf{u}^{(n)} - \mathbf{u}^{(s)}$ (green line); (middle) the number of vortex points per unit area in the channel (green dotted line), the number of positive vortex points per unit area (red line), the number of negative vortex points per unit area (black dotted line) and the polarization $\mathbf{p}$ (purple line); (right) the distribution of the positive (red) and negative (black) vortex points inside the channel once a statistically steady state has been achieved.

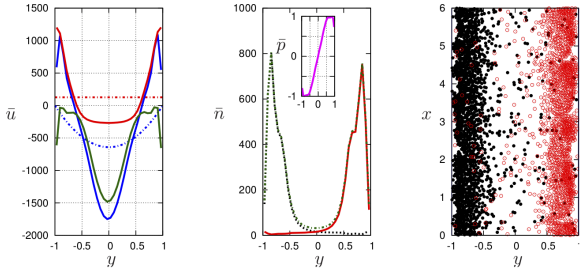

FIGURE 3. Numerical results for the extended two fluid model with low viscosity ($1/5$ of the above case): (left) the profile of superfluid component $\mathbf{u}^{(s)}$ (red line), the normal component $\mathbf{u}^{(n)}$ (blu line) compared with the Poiseuille profile (blue dotted line) and the counterflow velocity $\mathbf{u}^{(ns)} = \mathbf{u}^{(n)} - \mathbf{u}^{(s)}$ (green line); (middle) the number of vortex points per unit area in the channel (green dotted line), the number of positive vortex points per unit area (red line), the number of negative vortex points per unit area (black dotted line) and the polarization $\mathbf{p}$ (purple line); (right) the distribution of the positive (red) and negative (black) vortex points inside the channel once a statistically steady state has been achieved.

model obtained from the one-fluid extended model. The extended model is more general than the usual model because it predicts that the superfluid component carries a small amount of entropy and it is more thermodynamically consistent.

The numerical simulations performed in this paper first consider the two models with vortex-line densities consistent with Galantucci *et al.* (2017) and second employs the two-fluid extended model at very low viscosity. The results obtained from both models with

the same parameters agree with the experiments performed in Marakov *et al.* (2015). We have also emphasized that the profiles of the two components of superfluid helium have to be modified if we assume that the superfluid component can carry some amount of entropy, as reported in Putterman. In particular, the average velocity change according with $\overline{\mathbf{u}}^{(s)}_{s_s\neq 0} = 0.98\,\overline{\mathbf{u}}^{(s)}$ and $\overline{\mathbf{u}}^{(n)}_{s_s\neq 0} = 1.02\,\overline{\mathbf{u}}^{(n)}$, making the results closer to the experiments.

On the other hand, the low viscosity case considered in Subsection **3.2** emphasizes that the smaller viscosity makes the inertial and the mutual friction terms stronger causing the results shown in Fig. 3. In particular, the mutual friction term moves the vortex points apart with a resulting vanishing magnitude in the middle of the channel and very large in the proximity of the walls. This produces the observed normal fluid velocity profile, given that the normal fluid volume flow rate is constant, being determined by the constant heat released by the heater.

Furthermore, the inertial term contributes to the steepness of the profile of the normal component because nonlinearity becomes stronger than the viscous term, which fosters the leveling of the velocity profile.

Acknowledgments

This work was supported by National Group of Mathematical Physics (GNFM-INdAM). LG is supported by the Engineering and Physical Sciences Research Councile (EPSRC), grant n. EP/R005192/1. D.J. acknowledges the financial support from the Dirección General de Investigación of the Spanish Ministry of Economy and Competitiveness under grant TEC2015-67462-C2-2-R and of the Direcció General de Recerca of the Generalitat of Catalonia, under grant 2017 SGR-1018 and to Consolider Program Nanotherm (grant CSD-2010-00044) of the Spanish ministry of Science and Innovation.

References

Atkin, R. and Fox, N. (1984). "The dependence of thermal shock wave velocity on heat flux in helium II". *Journal of Physics C: Solid State Physics* **17**(7), 1191–1198. DOI: 10.1088/0022-3719/17/7/013.

Babuin, S., Stammeier, M., Varga, E., Rotter, M., and Skrbek, L. (2012). "Quantum turbulence of bellows-driven 4 He superflow: Steady state". *Physical Review B* **86**(13), 134515 [11pages]. DOI: 10.1103/PhysRevB.86.134515.

Babuin, S., Varga, E., Vinen, W. F., and Skrbek, L. (2015). "Quantum turbulence of bellows-driven He 4 superflow: Decay". *Physical Review B* **92**(18), 184503 [12pages]. DOI: 10.1103/PhysRevB.92.184503.

Barenghi, C. F., Donnelly, R. J., and Vinen, W. F. (2001). *Quantized Vortex Dynamics and Superfluid Turbulence*. Springer, berlin. DOI: 10.1007/3-540-45542-6.

Barenghi, C. F., Donnelly, R. J., and Vinen, W. (1983). "Friction on quantized vortices in helium II. A review". *Journal of Low Temperature Physics* **52**(3-4), 189–247. DOI: 10.1007/BF00682247.

Donnelly, R. (1991). *Quantized vortices in helium II*. Cambridge University Press.

Galantucci, L., Barenghi, C. F., Sciacca, M., Quadrio, M., and Luchini, P. (2011). "Turbulent superfluid profiles in a counterflow channel". *Journal of Low Temperature Physics* **162**(3-4), 354–360. DOI: 10.1007/s10909-010-0266-4.

Galantucci, L. and Sciacca, M. (2012). "Turbulent superfluid profiles and vortex density waves in a counterflow channel". *Acta applicandae mathematicae* **122**(1), 407–418. DOI: 10.1007/s10440-012-9752-9.

Galantucci, L. and Sciacca, M. (2014). "Non-classical velocity statistics in counterflow quantum turbulence". *Acta Applicandae Mathematicae* **132**(1), 273–281. DOI: 10.1007/s10440-014-9902-3.

Galantucci, L., Sciacca, M., and Barenghi, C. F. (2017). "Large-scale normal fluid circulation in helium superflows". *Physical Review B* **95**(1), 014509 [5pages]. DOI: 10.1103/PhysRevB.95.014509.

Galantucci, L., Sciacca, M., and Barenghi, C. F. (2015). "Coupled normal fluid and superfluid profiles of turbulent helium II in channels". *Physical Review B* **92**(17), 174530. DOI: 10.1103/PhysRevB.92.174530.

Hall, H. E. and Vinen, W. F. (1956). "The rotation of liquid helium II II. The theory of mutual friction in uniformly rotating helium II". *Proceedings of the Royal Society of London A* **238**(1213), 215–234. DOI: 10.1098/rspa.1956.0215.

Jou, D., Casas-Vàzquez, J., and Criado-Sancho, M. (2011). *Thermodynamics of Fluids Under Flow*. Springer. DOI: 10.1007/978-94-007-0199-1.

Jou, D., Casas-Vàzquez, J., and Lebon, G. (2010). *Extended Irreversible Thermodynamics*. Springer-Verlag. DOI: 10.1007/978-3-642-97671-1_2.

Jou, D. and Sciacca, M. (2013). "Quantum Reynolds number for superfluid counterflow turbulence". In: *Bollettino di Matematica Pura e Applicata*. Ed. by M. Mongiovì, M. Sciacca, and S. Triolo. Vol. VI. Palermo: Aracne editrice, pp. 95–103.

Keys, R. (1981). "Cubic convolution interpolation for digital image processing". *IEEE transactions on acoustics, speech, and signal processing* **29**(6), 1153–1160. DOI: 10.1109/TASSP.1981.1163711.

Khalatnikov, I. M. (2018). *An introduction to the theory of superfluidity*. CRC Press. DOI: 10.1201/9780429502897.

Landau, L. (1941). "Theory of the Superfluidity of Helium II". **60**(4), 356–358. DOI: 10.1103/PhysRev.60.356.

Lebon, G. and Jou, D. (1979). "A continuum theory of liquid helium II based on the classical theory of irreversible processes". *Journal of Non-Equilibrium Thermodynamics* **4**(5), 259–276. DOI: 10.1515/jnet.1979.4.5.259.

Lebon, J., Jou, D., and Casas-Vàzquez, J. (2008). *Understanding non-equilibrium thermodynamics*. Springer. DOI: 10.1007/978-3-540-74252-4.

London, F. (1954). *Superfluids*. Wiley.

Marakov, A., Gao, J., Guo, W., Van Sciver, S. W., Ihas, G. G., McKinsey, D. N., and Vinen, W. (2015). "Visualization of the normal-fluid turbulence in counterflowing superfluid He 4". *Physical Review B* **91**(9), 094503 [5pages]. DOI: 10.1103/PhysRevB.91.094503.

Mongiovì, M. S. (1991). "Superfluidity and entropy conservation in extended thermodynamics". *Journal of Non-Equilibrium Thermodynamics* **16**, 225–240. DOI: 10.1515/jnet.1991.16.3.225.

Mongiovì, M. S. (1992). "Thermomechanical Phenomena in Extended Thermodynamics of an Ideal Monoatomic Superfluid". *Journal of Non-Equilibrium Thermodynamics* **17**(2), 183–190. DOI: 10.1515/jnet.1992.17.2.183.

Mongiovì, M. S. (1993a). "Dissipation in an ideal monoatomic superfluid". *Journal of Non-Equilibrium Thermodynamics* **18**(1), 19–38. DOI: 10.1515/jnet.1993.18.1.19.

Mongiovì, M. S. (1993b). "Extended irreversible thermodynamics of liquid helium II". *Physical Review B* **48**(9), 6276–6283. DOI: 10.1103/PhysRevB.48.6276.

Mongiovì, M. S. (1993c). "The link between heat flux and stress deviator in extended thermodynamics of an ideal monoatomic superfluid". *Journal of Non-Equilibrium Thermodynamics* **18**(2), 147–156. DOI: 10.1515/jnet.1993.18.2.147.

Mongiovì, M. S. (2000). "Nonlinear extended thermodynamics of a non-viscous fluid in the presence of heat flux". *Journal of Non-Equilibrium Thermodynamics* **25**(1), 31–47. DOI: 10.1515/JNETDY.2000.003.

Mongiovì, M. S. (2001). "Extended irreversible thermodynamics of liquid helium II: boundary condition and propagation of fourth sound". *Physica A: Statistical Mechanics and its Applications* **292**(1–4), 55–74. DOI: 10.1016/S0378-4371(00)00537-9.

Mongiovì, M. S., Jou, D., and Sciacca, M. (2018). "Non-equilibrium thermodynamics, heat transport and thermal waves in laminar and turbulent superfluid helium". *Physics Reports* **726**, 1–71. DOI: 10.1016/j.physrep.2017.10.004.

Mueller, I. and Ruggeri, T. (1998). *Rational Extended Thermodynamics*. Springer-Verlag. DOI: 10.1007/978-1-4612-2210-1.

Nemirovskii, S. K. (2013). "Quantum turbulence: Theoretical and numerical problems". *Physics Reports* **524**(3), 85–202. DOI: 0.1016/j.physrep.2012.10.005.

Putterman, S. J. (1974). *Superfluid hydrodynamics*. American Elsevier Pub. Co.

Schwarz, K. W. (1988). "Three-dimensional vortex dynamics in superfluid He 4: Homogeneous superfluid turbulence". *Physical Review B* **38**(4), 2398–2417. DOI: 10.1103/PhysRevB.38.2398.

Sciacca, M., Sellitto, A., and Jou, D. (2014). "Transition to ballistic regime for heat transport in helium II". *Physics Letters A* **378**(34), 2471–2477. DOI: 10.1016/j.physleta.2014.06.041.

Tisza, L. (1938). "Transport phenomena in helium II". *Nature* **141**(3577), 913. DOI: 10.1038/141913a0.

Varga, E., Babuin, S., and Skrbek, L. (2015). "Second-sound studies of coflow and counterflow of superfluid 4He in channels". *Physics of Fluids* **27**(6), 065101 [22pages]. DOI: 10.1063/1.4921816.

Vinen, W. F. (1957a). "Mutual friction in a heat current in liquid helium II I. Experiments on steady heat currents". *Proceedings of the Royal Society of London A* **240**(1220), 114–127. DOI: 10.1098/rspa.1957.0071.

Vinen, W. F. (1957b). "Mutual friction in a heat current in liquid helium II III. Theory of the mutual friction". *Proceedings of the Royal Society of London A* **242**(1231), 493–515. DOI: 10.1098/rspa.1957.0191.

Vinen, W. F. (1957c). "Mutual friction in a heat current in liquid helium II. II. Experiments on transient effects". *Proceedings of the Royal Society of London A* **240**(1220), 128–143. DOI: 10.1098/rspa.1957.0072.

Vinen, W. (1958). "Mutual friction in a heat current in liquid heliumn. II. IV. Critical heat currents in wide channels". *Proceedings of the Royal Society of London A* **243**(1234), 400–413. DOI: 10.1098/rspa.1958.0007.

[a] Joint Quantum Centre (JQC) Durham–Newcastle and School of Mathematics and Statistics
Newcastle University, Newcastle upon Tyne
NE1 7RU, United Kingdom

[b] Università degli Studi di Palermo
Dipartimento di Scienze Agrarie e Forestali
Viale delle Scienze, 90128 Palermo, Italy

[c] Istituto Nazionale di Alta Matematica (INDAM)
Roma 00185 , Italy

[d] Universitat Autònoma de Barcelona,
Departament de Física,
Bellaterra, Catalonia, Spain

[e] Institut d'Estudis Catalans
Carme 47, Barcelona 08001,
Catalonia, Spain

[*] To whom correspondence should be addressed | email: michele.sciacca@unipa.it

Paper contributed to the international workshop entitled "New approaches to study complex systems",
which was held in Messina, Italy (27–28 november 2017), under the patronage of the *Accademia Peloritana dei Pericolanti*
Manuscript received 17 October 2018; published online 20 December 2019